

# Direct Observation of Lithium Staging in Partially Delithiated $\text{LiFePO}_4$ at Atomic Resolution

Lin Gu,<sup>\*,†,§</sup> Changbao Zhu,<sup>‡</sup> Hong Li,<sup>\*,§</sup> Yan Yu,<sup>‡</sup> Chilin Li,<sup>‡</sup> Susumu Tsukimoto,<sup>†</sup> Joachim Maier,<sup>‡</sup> and Yuichi Ikuhara<sup>†,||,⊥</sup>

<sup>†</sup>WPI Advanced Institute for Materials Research, Tohoku University, Sendai 980 8577, Japan

<sup>‡</sup>Max Planck Institute for Solid State Research, Stuttgart 70569, Germany

<sup>§</sup>Institute of Physics, Chinese Academy of Sciences, Beijing 100190, P. R. China

<sup>||</sup>Nanostructures Research Laboratory, Japan Fine Ceramic Centre, Nagoya, 456-8587, Japan

<sup>⊥</sup>Institute of Engineering Innovation, the University of Tokyo, Tokyo, 113-8656, Japan

**S** Supporting Information

**ABSTRACT:** Lithium ions in  $\text{LiFePO}_4$  were observed directly at atomic resolution by an aberration-corrected annular-bright-field scanning transmission electron microscopy technique. In addition, it was found in partially delithiated  $\text{LiFePO}_4$  that the remaining lithium ions preferably occupy every second layer, along the  $b$  axis, analogously to the staging phenomenon observed in some layered intercalation compounds. This new finding challenges previously proposed  $\text{LiFePO}_4/\text{FePO}_4$  two-phase separation mechanisms.

It is lens aberrations which limit the attainable spatial resolution of a transmission electron microscope (TEM) to usually 50 times the wavelength of the fast electrons. The incorporation of an aberration corrector to a TEM established a milestone concerning both atomically resolved microscopy and spectroscopy,<sup>1</sup> so that operationally complicated and computationally expensive methods, such as focal-series reconstruction which was applied previously to resolve Li columns in  $\text{LiCoO}_2$ ,<sup>2</sup> are no longer indispensable. The recent success in aberration-corrected annular-bright-field (ABF) scanning transmission electron microscopy (STEM) provides a feasible access to a direct interpretation of the atomic structure at subangstrom resolution. Such a procedure is highly efficient in resolving atomic columns, particularly for light elements, without a stringent specimen thickness requirement.<sup>3</sup> ABF has been applied to observe lithium ions in spinel-structured  $\text{LiMn}_2\text{O}_4$  and  $\text{LiV}_2\text{O}_4$  so far.<sup>4</sup> Here we demonstrate that this technique can be further extended to observe lithium ions directly in olivine-type lithium iron phosphate ( $\text{LiFePO}_4$ ).

$\text{LiFePO}_4$  was first reported by Pahdi et al. as a positive electrode material in lithium ion batteries.<sup>5</sup> The intrinsic low electronic conductivity<sup>6</sup> and poor ionic transport property<sup>7</sup> are the limiting factors to achieving high rate performances. Decreasing the particle size<sup>8</sup> and applying a carbon coating<sup>9</sup> were demonstrated to be very effective strategies for improving the kinetic properties of  $\text{LiFePO}_4$ . Modified  $\text{LiFePO}_4$  shows promising features as a cathode active material in lithium ion batteries for hybrid electric vehicles and stationary energy storage

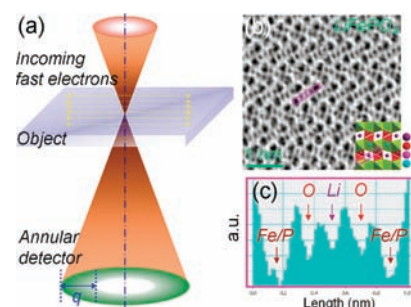


**Figure 1.** (a) Schematic of the annular-bright-field (ABF) imaging geometry. A demonstration of lithium sites within a  $\text{LiFePO}_4$  crystal is shown in (b) with the corresponding line profile acquired at the box region shown in (c) to confirm the lithium contrast with respect to oxygen.

batteries. Despite the great success in practical applications, the microscopic mechanism of the phase transition from  $\text{LiFePO}_4$  to  $\text{FePO}_4$  is still under debate. Core–shell,<sup>5</sup> mosaic,<sup>10</sup> shrinking-core,<sup>11</sup> domino-cascade,<sup>12</sup> phase transformation wave,<sup>13</sup> and many particle models<sup>14</sup> have been proposed. Obviously, acquiring direct images of  $\text{LiFePO}_4$  and partially delithiated  $\text{LiFePO}_4$  at atomic resolution is essential to clarify the above question. Based on an annular-dark-field (ADF) collection geometry, Cs-corrected STEM was used so far to detect the presence of antisite Fe ions (i.e., Fe ions on Li sites) in  $\text{LiFePO}_4$ , a method that is not yet capable of resolving Li ions directly.<sup>15</sup>

Figure 1 shows a scheme of the ABF imaging geometry, in which a fine probe with a spot size less than 1 Å scans across the specimen. An annular detector is placed at the post column, defining a collection semiangle between 11 to 20 mrad. The advantage of this collection geometry is readily envisaged in comparison to normal bright-field acquisition that the optical-axis collection, corresponding to the phase contrast conventional high resolution imaging condition, is modified to a semicoherent imaging regime.<sup>3,16</sup> Consequently, the ABF electron micrograph of pure phase  $\text{LiFePO}_4$  in Figure 1b directly reveals the lithium atomic sites with the corresponding structural schematic shown

**Received:** October 19, 2010

**Published:** March 10, 2011

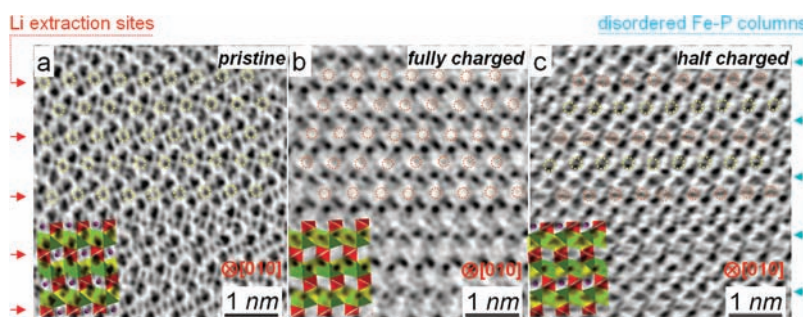


**Figure 2.** ABF micrographs showing Li ions of partially delithiated  $\text{LiFePO}_4$  at every other row. (a) Pristine material with the atomic structure of  $\text{LiFePO}_4$  shown as inset; (b) fully charged state with the atomic structure of  $\text{FePO}_4$  shown for comparison; and (c) half charged state showing the Li staging. Note that Li sites are marked by yellow circles and the delithiated sites are marked by orange circles.

in the inset. Detailed contrast analyses by the line profile (shown in Figure 1c) acquired at the box region (see both ABF micrograph and structural schematic) confirmed the lithium contrast in comparison to that of oxygen, indicating a  $Z^{1/3}$  contrast dependence with respect to the atomic number.<sup>3</sup> The intensity from O, P, and Fe is shown as well for comparison. Note that the columns of Fe, P, and part of O cannot be distinguished due to the overlapping of the relatively large atomic radii along the [010] projection.

The  $\text{LiFePO}_4$  sample was prepared by an electrospinning method. The phase purity is demonstrated in the X-ray diffraction (XRD) patterns (Figure S1) with the corresponding nanowire morphology ( $d = 65$  nm) shown in Figure S2. The charging voltage profile is typical for  $\text{LiFePO}_4$  (see galvanostatic intermittent titration technique curves in Figure S3). The half-delithiated  $\text{Li}_{0.5}\text{FePO}_4$  was obtained by an electrochemical method. The charge and discharge cycling was carried out twice at 0.1C (10 h to fully charge or discharge), and then the battery was charged for 5 h to prepare half-delithiated  $\text{LiFePO}_4$ . The battery was disassembled in the glovebox under an argon atmosphere, and the active materials on the Al current collector were washed by anhydrous DMC several times for further characterization. TEM specimens were prepared by drop-coating the materials individually onto carbon lacey films approximately one week after the electrochemical treatment, which were further aligned in the microscope at the desired orientation via precise goniometry control. Electron energy-loss spectroscopy (EELS) results after charging indicate a systematic alteration of the Fe valence from  $2^+$  to  $3^+$  (see EELS of pristine, half-charged, and charged  $\text{LiFePO}_4$  in Figure S4).

Figure 2c shows an ABF micrograph of partially delithiated  $\text{LiFePO}_4$  ( $\sim 0.5$  mol of Li is delithiated) acquired from the [010] axis (space group  $Pnma$ ). In comparison to the pristine material shown in Figure 2a, in which the lithium sites are marked by yellow circles, part of the lithium remains in the lattice after charging at every other row as labeled by yellow circles in Figure 2c. The Li-extraction sites are indicated by red arrows. Schemes of the  $\text{LiFePO}_4$  and  $\text{Li}_{0.5}\text{FePO}_4$  structures are shown in the inset, respectively. Note that, within the unit cell where lithium ions are extracted, the upper nearby Fe–P columns, as indicated by cyan arrows, render a fuzzy contrast indicating a disordering of the local structure: i.e., the atoms no longer occupy the original position by a small deviation of  $r - r_0$ , so that the electron channelling effect fails to hold. We believe this is highly likely to be related to the  $\text{LiFePO}_4$  delithiation process. Consequently, a faint contrast corresponding to diffused O columns is observed close to the vacant places in the rows where Li ions are extracted. This can

be associated with the above-mentioned Fe–P column distortion. Note that the ABF micrograph of fully charged  $\text{FePO}_4$  with the corresponding structural schematic is shown in Figure 2b for reference, in which the distortion of the Fe–P column vanishes in association with a more diffused O distribution around the  $\text{LiO}_6$  octahedra. A detailed contrast comparison for lithiated and delithiated states is displayed in Figure S5.

The high resolution atomic image shows clearly that a first-order lithium staging structure exists for the partially delithiated  $\text{Li}_{1-x}\text{FePO}_4$  ( $x \approx 0.5$ ) samples. Such a microstructure has not been observed by a normal HRTEM technique<sup>12,18</sup> or by other techniques.<sup>19</sup> The appearance of a staging structure in  $\text{Li}_{1-x}\text{FePO}_4$  is certainly not consistent with a simple two-phase separation model.<sup>5,10–14</sup> The formation of the staging structure is well-known in graphite intercalation compounds<sup>20</sup> and some other layer compounds, i.e.,  $\text{TiS}_2$ .<sup>21</sup> The origin of the staging formation could be driven by the existence of elastic coherence strain and minimization of the Li–Li repulsive interaction.<sup>22</sup> It is not clear whether the staging phenomenon refers to a thermodynamically stable or metastable situation in nanosized samples. Further theoretical and experimental clarification should be undertaken to clarify the formation mechanism in such an olivine structure compound and the decisive factors for the formation of the lithium staging, such as size, morphology, and charging rate. Nevertheless, the current result shows that lithium extraction from a well studied two-phase transition system could be different from typical behaviors of bulk material in an equilibrium state. Obviously, a clear structural evolution picture of other important lithium-containing electrodes could also be disclosed now at atomic resolution based on the ABF technique which is indeed essential to understand Li-storage mechanisms in important energy storage materials and other materials containing small and light elements.

## ■ ASSOCIATED CONTENT

**S** Supporting Information. Material preparation; remarks on radiation damage; electrochemical analyses of the capacity versus voltage for the cell under investigation; XRD comparison of the charged state of  $\text{LiFePO}_4$  and the pristine material; high-resolution transmission electron micrograph (HRTEM) reveals the pristine  $\text{LiFePO}_4$  lattice with the corresponding diffraction shown in the inset; EELS comparison of the pristine, half charged and fully charged  $\text{LiFePO}_4$ ; and detailed ABF contrast analyses. This information is available free of charge via Internet at <http://pubs.acs.org>.

## AUTHOR INFORMATION

## Corresponding Author

gu@wpi-aimr.tohoku.ac.jp; hli@iphy.ac.cn

## ACKNOWLEDGMENT

We acknowledge the financial support from Japan Society for the Promotion of Science (JSPS) Grant-in-Aid for Young Scientists reference 22760506. Part of this research was supported by the JSPS through its "Funding program for World-Leading Innovative R&D on Science and Technology (FIRST Program)". We are grateful to Katja Weichert for helpful discussions. L.G. is grateful for the support from the "Hundred Talents" program of the Chinese Academy of Sciences. We acknowledge the financial support from the "863" Project (2009AA033101).

## REFERENCES

- (1) (a) Haider, M.; Uhlemann, S.; Schwan, E.; Kabius, B.; Urban, K. *Nature* **1998**, *392*, 768–769. (b) Batson, P. E.; Dellby, N.; Krivanek, O. L. *Nature* **2002**, *418*, 617–620.
- (2) Shao-Horn, Y.; Croguennec, L.; Delmas, C.; Nelson, E. C.; O'Keefe, M. A. *Nat. Mater.* **2003**, *2*, 464–467.
- (3) (a) Findlay, S. D.; Shibata, N.; Sawada, H.; Okunishi, E.; Kondo, Y.; Yamamoto, T.; Ikuhara, Y. *Appl. Phys. Lett.* **2009**, *95*, 191913. (b) Findlay, S. D.; Shibata, N.; Sawada, H.; Okunishi, E.; Kondo, Y.; Ikuhara, Y. *Ultramicroscopy* **2010**, *110*, 903–923.
- (4) (a) Huang, R.; Ikuhara, Y. H.; Moriwake, H.; Kuwabara, A.; Fisher, C. A. J.; Ikuhara, Y.; Mizoguchi, T.; Oki, H. *Proceedings of the 22nd Fall Meeting of the Ceramic Society of Japan*; 2009; p 300, ISBN 978-4-931298-56-9. (b) Oshima, Y.; Sawada, H.; Hosokawa, F.; Okunishi, E.; Kaneyama, T.; Kondo, Y.; Niitaka, S.; Takagi, H.; Tanishiro, Y.; Takayanagi, K. *J. Electron Microsc.* **2010**, *59*, 457–461. (c) Huang, R.; Ikuhara, Y. H.; Mizoguchi, T.; Findlay, S. D.; Kuwabara, A.; Fisher, C. A. J.; Moriwake, H.; Oki, H.; Hirayama, T.; Ikuhara, Y. *Angew. Chem.*, in press.
- (5) Padhi, A.; Goodenough, J. B. *J. Electrochem. Soc.* **1997**, *144*, 1188–1194.
- (6) (a) Delacourt, C.; Laffont, L.; Bouchet, R.; Wurm, C.; Leriche, J. B.; Morcette, M.; Tarascon, J. M.; Masquelier, C. *J. Electrochem. Soc.* **2005**, *152*, A913–A921. (b) Yonemura, M.; Yamada, A.; Takei, Y.; Sonoyama, N.; Kanno, R. *J. Electrochem. Soc.* **2004**, *151*, A1352–A1356. (c) Molenda, J.; Ojczyk, W.; Swierczek, K.; Zajac, W.; Krok, F.; Dygas, J.; Liu, R. S. *Solid State Ionics* **2006**, *177*, 2617–2624.
- (7) (a) Prosini, P. P.; Lisi, M.; Zane, D.; Pasquali, M. *Solid State Ionics* **2002**, *148*, 45–51. (b) Amin, R.; Balaya, P.; Maier, J. *Electrochem. Solid State Lett.* **2007**, *10*, A13–A16. (c) Amin, R.; Maier, J. *Solid State Ionics* **2008**, *178*, 1831–1836. (d) Amin, R.; Lin, C. T.; Maier, J. *Phys. Chem. Chem. Phys.* **2008**, *10*, 3519–3523. (e) Amin, R.; Lin, C. T.; Maier, J. *Phys. Chem. Chem. Phys.* **2008**, *10*, 3524–3529.
- (8) (a) Yamada, A.; Chung, S. C.; Hinokuma, K. *J. Electrochem. Soc.* **2001**, *148*, A224–A229. (b) Yang, S. F.; Zavalij, P. Y.; Whittingham, M. S. *Electrochem. Commun.* **2001**, *3*, 505–508. (c) Yang, S. F.; Song, Y. N.; Zavalij, P. Y.; Whittingham, M. S. *Electrochem. Commun.* **2002**, *4*, 239–244. (d) Delacourt, C.; Poizot, P.; Levasseur, S.; Masquelier, C. *Electrochem. Solid State Lett.* **2006**, *9*, A352–A355. (e) Bakkenov, Z.; Taniguchi, I. *Electrochem. Commun.* **2010**, *12*, 75–78.
- (9) (a) Ravet, N.; Goodenough, J. B.; Besner, S.; Simoneau, M.; Hovington, P.; Armand, M.; *Electrochem. Soc. Meet. Abstr.* **1999**, *196*, No.127. (b) Huang, H.; Yin, S. C.; Nazar, L. F. *Electrochem. Solid State Lett.* **2001**, *4*, A170–A172. (c) Chen, Z.; Dahn, J. R. *J. Electrochem. Soc.* **2002**, *149*, A1184–A1189. (d) Dominko, R.; Bele, M.; Gaberscek, M.; Remskar, M.; Hanzel, D.; Jamnik, J. *J. Electrochem. Soc.* **2005**, *152*, A858–A863. (e) Li, G. H.; Azuma, H.; Tohda, M. *Electrochem. Solid State Lett.* **2002**, *5*, A135–A137. (f) Gaberscek, M.; Dominko, R.; Bele, M.; Remskar, M.; Hanzel, D.; Jamnik, J. *Solid State Ionics* **2005**, *176*, 1801–1805.
- (10) (a) Andersson, A. S.; Kalska, B.; Haggstrom, L.; Thomas, J. O. *Solid State Ionics* **2000**, *130*, 41–52. (b) Andersson, A. S.; Thomas, J. O. *J. Power Sources* **2001**, *97–98*, 498–502.
- (11) Srinivasan, V.; Newman, J. *J. Electrochem. Soc.* **2004**, *151*, A1517.
- (12) Delmas, C.; Maccario, M.; Croguennec, L.; Le Cras, F.; Weill, F. *Nat. Mater.* **2008**, *7*, 665–671.
- (13) (a) Burch, D.; Singh, G.; Ceder, G.; Bazant, M. Z. *Solid State Phenomena* **2008**, *139*, 95–100. (b) Singh, G. K.; Ceder, G.; Bazant, M. Z. *Electrochim. Acta* **2008**, *53*, 7599–7613.
- (14) Dreyer, W.; Jamnik, J.; Guhlke, C.; Huth, R.; Moškon, J.; Gabersček, M. *Nat. Mater.* **2010**, *9*, 448–453.
- (15) (a) Chung, S. Y.; Choi, S. Y.; Yamamoto, T.; Ikuhara, Y. *Phys. Rev. Lett.* **2008**, *100*, 125502. (b) Chung, S. Y.; Choi, S. Y.; Yamamoto, T.; Ikuhara, Y. *Angew. Chem., Int. Ed.* **2009**, *48*, S43–S46.
- (16) Rose, H. *Ultramicroscopy* **1977**, *2*, 251–267.
- (17) Zhu, C. B.; Yu, Y.; Gu, L.; Weichert, K.; Maier, J. To be published.
- (18) (a) Chen, G.; Song, X.; Richardson, T. J. *Electrochem. Solid State Lett.* **2006**, *9*, A295–A298. (b) Laffont, L.; Delacourt, C.; Gibot, P.; Wu, M. Y.; Kooyman, P.; Masquelier, C.; Tarascon, J. M. *Chem. Mater.* **2006**, *18*, 5520–5529.
- (19) (a) Delacourt, C.; Poizot, P.; Tarascon, J. M.; Masquelier, C. *Nat. Mater.* **2005**, *4*, 254–260. (b) Pierre, G.; Montse, C. C.; Lydia, L.; Stephane, L.; Philippe, C.; Stephane, H.; Tarascon, J. M.; Masquelier, C. *Nat. Mater.* **2008**, *7*, 741–747. (c) Sigle, W.; Amin, R.; Weichert, K.; van Aken, P. A.; Maier, J. *Electrochem. Solid State Lett.* **2009**, *12*, A151–A154.
- (20) Fischer, J. E.; Tompson, T. E. *Phys. Today* **1977**, *31*, 36.
- (21) (a) Fernandez-Moran, H.; Ohstuki, M.; Hibino, A.; Hough, C. *Science* **1971**, *174*, 498–500. (b) Soreau, A.; Danot, M.; Trichet, L.; Rouxel, J. *Mater. Res. Bull.* **1974**, *9*, 191.
- (22) (a) Safran, S. A.; Hamann, D. R. *Phys. Rev. Lett.* **1979**, *42*, 1410–1413. (b) Safran, S. A.; Hamann, D. R. *Phys. Rev.* **1980**, *22*, 606–612.